A finite-element-based reverse identification of DC conductivity based on leakage current measurements on miniature cables

Adrien **CHARMETANT**, Dimitri **CHARRIER**, Jean-Hugues **DOUMBE**, Arnaud **ALLAIS**; Nexans, Lyon, France, adrien.charmetant@nexans.com, dimitri.charrier@nexans.com, jean-hugues.doumbe@nexans.com, arnaud.allais@nexans.com

ABSTRACT

DC leakage current measurements on miniature cables are presented. Two approaches are proposed to deduce the DC electrical conductivity of the tested insulation material from these measurements: one approach based on an assumed electric field value in the insulation, and a coupled LMA-FEM approach which does not require this assumption. It is shown that using a-priori electric field values leads to significant mistakes on the identified DC conductivities, which can lead to underestimated DC conductivities.

KEYWORDS

HVDC, leakage current, electrical conductivity, finite-element simulation

INTRODUCTION

In the context of the land power transmission, the technology of direct current at high voltage (HVDC) offers many technical and commercial advantages over AC technology [1].

The electrical conductivity and its variation with temperature, electric field and by-products content are of key importance to assess the stability and the performance of an HVDC insulation system in rated condition and in test condition according to CIGRE recommendations.

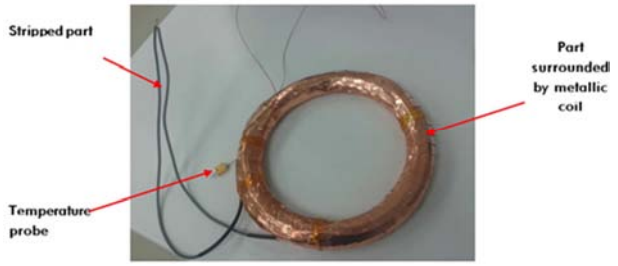

Fig. 1: Miniature cable coil used for leakage current measurements

This paper presents how the measurement of leakage currents through miniature cables insulations has been optimized to avoid biases due to surface currents coming from the termination.

In order to estimate the electrical conductivity from these measurements, two approaches are then proposed. The first approach uses a-priori assumption of the electric field distribution in the miniature cable. The second approach, more complex but also more versatile, does not need this assumption as it uses a coupling between an optimization algorithm and a finite-element model. It is shown how sensitive the results are to the reverse identification used.

LEAKAGE CURRENT MEASUREMENTS ON CABLES

Neither the electrical conductivity of a material nor the electric field distribution in a sample can be directly measured. Therefore, the law describing the electrical conductivity as a function of the electric field and the temperature must be calculated from current, voltage and temperature measurements.

A measurement methodology of leakage currents through the insulation in a miniature cable has been reported [2]. The inner and outer semiconductor radiuses are 1.4 mm and 2.9 mm respectively. In this method a 30-meter long coil of miniature cable is used (see Fig. 1). Using such a large length allows obtaining accurately measureable currents. This coil is surrounded by a copper tape which collects the current flowing through the insulations.

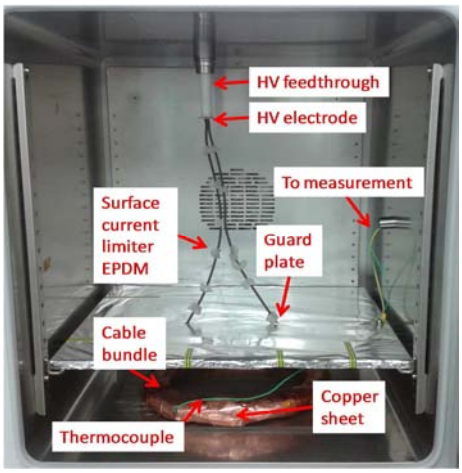

Fig. 2: Picture of the leakage current measurement bench

As shown in Fig. 2, the leakage current measurement consists in applying a high voltage (HV) in the conductor of the cable and to ground its outer semiconductor which is covered by a copper sheet. The sheet is connected to the electrometer used as an ammeter. A LabVIEW interface allows driving these equipments and acquiring data. An oven is used, and a thermocouple probe is placed inside the cable bundle to monitor its temperature.

An equivalent schematic of the electrical part of the bench is showed in Fig. 3. As dynamic en transient phenomenon can take place during measurement, the cable is represented by a capacitance in parallel with a resistance that we want to estimate.

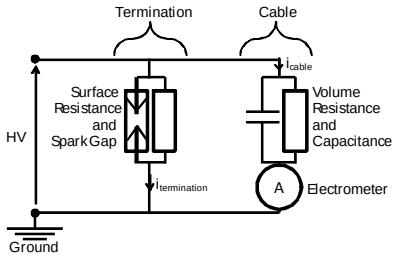

Fig. 3: Equivalent circuit of a set up for leakage current measurement on miniature cable

Past experiences showed that surface currents at the terminations are likely to appear: the termination behaves as a pure resistance in parallel with a spark-gap, which are both illustrated in Fig. 3. The resulting current is the superposition of a steady current and of current peaks (Fig. 4). The resistance can be increased by increasing the length (up to 50 cm) between the HV electrode and the outer screen and by adding rubber plots to increase the leakage path along the interface. The spark signals can be avoided in the electrometer by adding a guard electrode before the outer semiconductor. Implementing both solutions allowed drastically reducing the surface current contribution from the volume current.

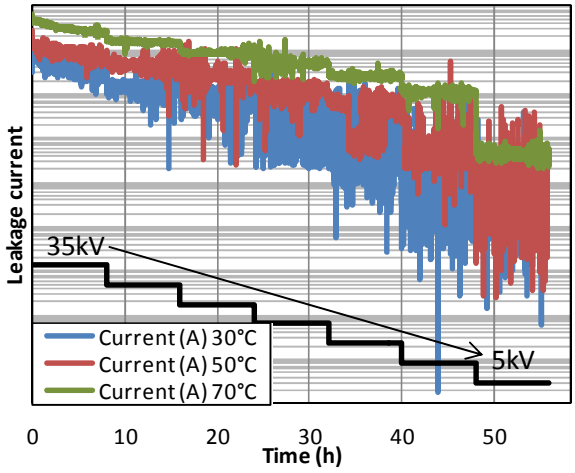

Fig. 4: Raw leakage current data obtained before optimization for a miniature cable under DC voltage

The set up for miniature cable allows reaching the windows of operating and testing temperatures and electric field in full size HVDC cables. Regarding the electric field, a voltage sequence was chosen with steps of 5 kV from high to lower voltages to reduce the impact of depolarization between each voltage values. Typically, a voltage on minicable of +/-35 kV gives a mean field of 22.4 kV.mm^{-1} equivalent to a maximal field in a 348 kV full size with 21 mm XLPE thickness.

The results consists of a set of currents, corresponding to the different temperatures and voltages imposed to the coil. An example of obtained raw data is shown in Fig. 4.

A specific numerical treatment allows reducing the noise, which is rather important for low temperatures and low voltages, to obtain a set of leakage currents depending on voltage and temperature, shown in Fig. 5.

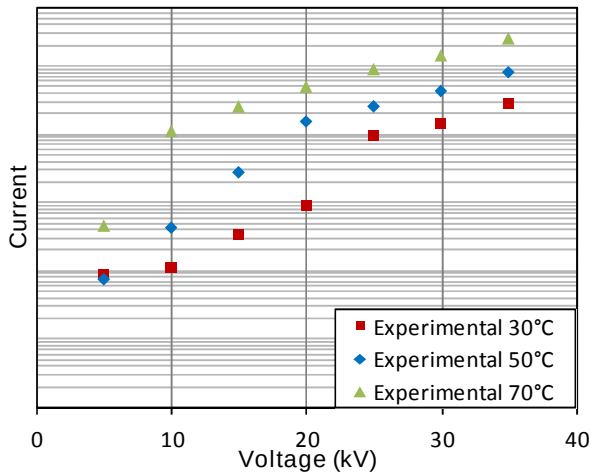

Fig. 5: Measure of the leakage current on a 30 m miniature cable as a function of voltage

In order to obtain the intrinsic electrical behavior of an insulation material, to compare the performances of different materials and to understand the influence of the manufacturing process on materials performances, the electrical conductivity must be extracted from these leakage current measurements.

FROM LEAKAGE CURRENT TO ELECTRICAL CONDUCTIVITY

The electrical conductivity of insulating materials is known to depend on the temperature and on the electric field [3-8]. Quantitative knowledge of these dependencies is of first order importance to estimate the performance of an HVDC insulation system [5,9,11]. The extraction of electrical conductivities from leakage current measurements is not obvious, mainly because the electric field distribution in the test object is not known.

Standard reverse identification approach

A common approximation of the electric field distribution in a cable is to assume that it is “purely Laplacian”, i.e. to consider that the electric field derives from an electric potential which is a solution of Laplace’s equation with no space charges and with constant electrical conductivity over the thickness. Considering a perfectly round insulation layer with constant thickness, which inner and outer radius are respectively r_i and r_o, submitted to an electric potential V, this approach leads to the following maximum electric field:

$$E = \frac{V}{r_i \cdot \ln(r_o / r_i)} \qquad [1]$$

With this approach, and for a measured leakage current I, the electrical conductivity can be calculated as [2]:

$$\sigma = \frac{I}{2\pi \cdot V} \ln(r_o / r_i) \qquad [2]$$

An example of conductivity result obtained from the previously presented current measurements on miniature cable and using this approach is given in Fig. 6.

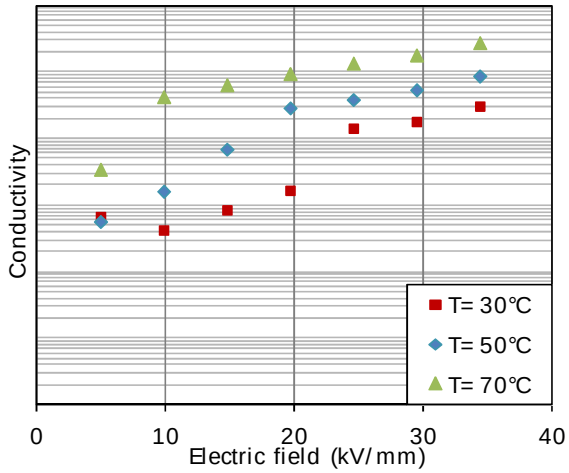

Fig. 6: Electrical conductivities obtained from leakage currents using the standard "Laplacian" approach

To be used in numerical simulation models, these conductivity values must be fitted, by assuming a behavior law to describe the evolution of the electrical conductivity depending on temperature, electric field, crosslinking by-products, microstructure, local defects or any other variable. In this work we chose to use the widely used following function:

$$\sigma(T,E) = \sigma_0 \exp(\alpha T)\exp(\beta E) \qquad [3]$$

This behavior law does not include the influence of the crosslinking by-products on the electrical conductivity, because the miniature cables used for the experiments had been very well degassed. Therefore the effect of potential residual by-products will be indirectly included in the σ_0 material constant. When this behavior law is used, a parameter vector with three components can be defined:

$$\vec{p} = \begin{pmatrix} \sigma_0 \\ \alpha \\ \beta \end{pmatrix} \qquad [4]$$

This parameter vector must be found by fitting the experimental data with the model. This fitting could be done with Excel's solver feature, but it was shown that Excel algorithm shows poor convergence when experimental data is scattered. Therefore, a Levenberg-Marquart algorithm (LMA) has been implemented and used to do this fitting. This algorithm is presented in the below subsection.

Levenberg-Marquardt Algorithm (LMA)

The LMA is an optimization algorithm, commonly used for non-linear least squares optimization problems such as curve fitting. It is an interpolation of the Gauss-Newton algorithm and the gradient descent method, which benefits from the advantages of both methods: it can find a solution even if it starts very far from the optimum, and converges quickly even near the optimum.

From the previously described measurements, we obtain a set of leakage currents I_n corresponding to an imposed voltage V_n and an imposed temperature T_n. This set will be denoted:

$$\vec{I}_{\exp} = \left\{ I^n_{\exp}\left(V_n, T_n\right) \right\}_{n=1..N} \qquad [5]$$

Through the test object model, using a vector of parameters $\vec{p}$, a set of leakage currents can be computationally obtained using the same voltages and temperatures:

$$\vec{I}_{simul}\left(\left\{V_n, T_n\right\}_{n=1..N}, \vec{p}\right) = \left\{ I^n_{simul}\left(V_n, T_n, \vec{p}\right) \right\}_{n=1..N} \qquad [6]$$

The function $\vec{f}$ represents the transformation operated by the numerical model of a set of voltages and temperatures and a vector parameter into a leakage current:

$$\vec{I}_{simul} = \vec{f}\left(\left\{V_n, T_n\right\}_{n=1..N}, \vec{p}\right) \qquad [7]$$

The LMA iteratively computes the parameter vector $\vec{p}$ so that the computed leakage currents fit with the experimentally obtained leakage currents. Mathematically, this statement can be expressed as a least-square minimization problem with the error function S:

$$S = \left\| \vec{I}_{\exp} - \vec{I}_{simul}\left(\vec{p}\right) \right\| = \sum_{n=1}^{N} \left(I^n_{\exp} - I^n_{simul}\left(\vec{p}\right) \right)^2 \qquad [8]$$

In the LMA iterative process, the following formula is used to compute the parameter vector at each iteration:

$$\vec{p}_{i+1} = \vec{p}_i + \left(\mathbf{J}^T \mathbf{J} + \lambda \mathbf{I} \right)^{-1} \mathbf{J}^T \left(\vec{I}_{\exp} - \vec{I}_{simul}\left(\vec{p}_i\right) \right) \qquad [9]$$

In this formula, $\vec{p}_i$ is the parameter vector at increment i, $\mathbf{J}$ is the Jacobian matrix of the function $\vec{f}$ and λ is a damping factor.

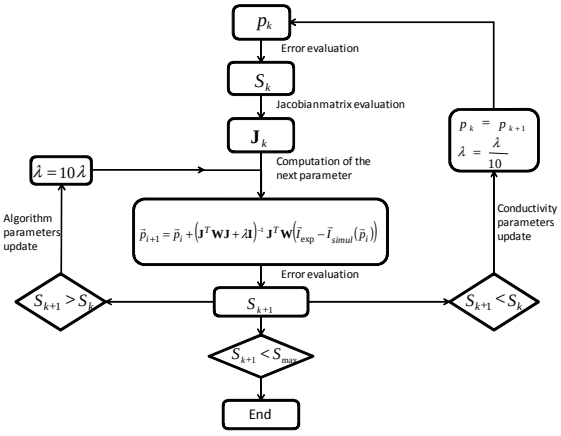

Fig. 7: Block diagram of the LMA

This algorithm has been implemented in Matlab, following the diagram of the Fig. 7.

Result of the fitting

The fitting obtained by using the previously presented experimental data, "purely laplacian" assumption, conductivity law and LMA algorithm, is shown on the Fig. 8.

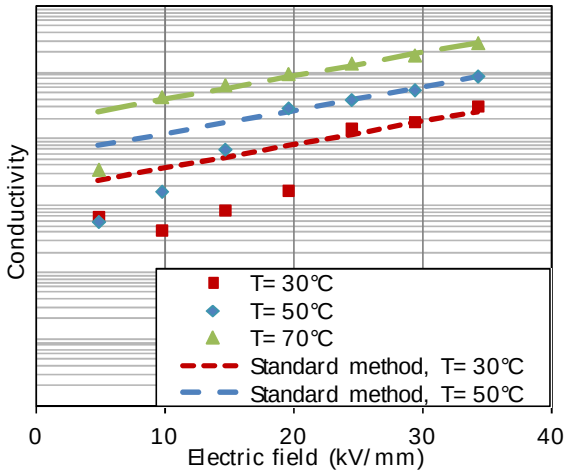

Fig. 8: Fitting obtained with the standard identification approach

This fitting allows obtaining a model which matches well the experimental data for high electric field values, but for low values the fitting is quite poor. This comes from the fact that conductivity changes are of several orders of magnitude, and therefore : the values for low electric fields have less weight in the error function defined in equation 8.

Recalculate the I(V) curve using a finite-elements model

A simplified, "purely laplacian" approach has been used for estimating the electric field in the insulation of the miniature cable. If this approach is correct, calculating an I(V) curve using a finite-element model implementing the previous fitting should return the same current values, at least for high electric field values for which the fitting works well. Therefore a finite-element model of the miniature cable has been developed, which is described thereafter.

It is assumed in this model that the miniature cable is perfectly straight, round, and shows axial symmetry. Its temperature is assumed homogeneous within the whole cross-section and length. Also, the conductor and the inner and outer semiconductive screens of the miniature cable are considered infinitely more electrically conductive than the insulation. With these assumptions, a simple 1D axially-symmetric model of the insulation has been setup, using Comsol Multiphysics software. The Fig. 9 shows the final modeled geometry.

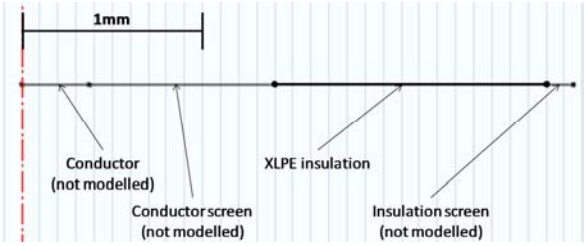

Fig. 9: 1D axial symmetric model of the miniature cable insulation

This geometry is discretized into small elements at which the electric field, the electric potential and the current density are calculated by solving Maxwell's equations.

The conductivity law of equation 3 is used with the parameters identified by the fitting procedure.

The Fig. 10 compares the I(V) curves obtained with this model with the experimental I(V) curves. It is clear that despite their apparent good fitting, the conductivity parameters identified does not allow obtaining good leakage currents for high-electrical-field values.

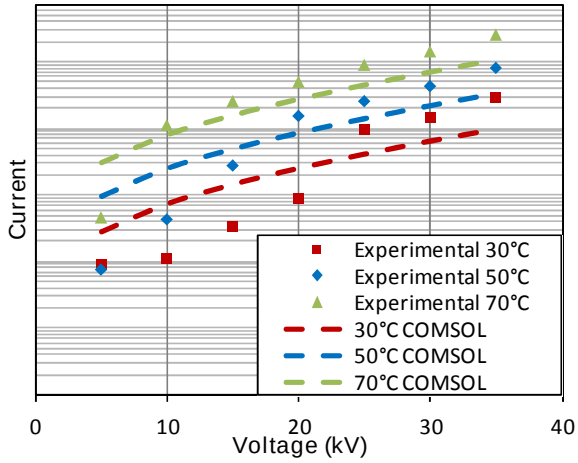

Fig. 10: I(V) curves obtained using the finite element model with the results of the standard identification method

It is well-known that space charges accumulation can happen in HVDC insulation materials [11-14] and that the electrical conductivity variations with field and temperature [3-8] induce changes in the electrical field distribution.

The previous results show that considering the electric field as being purely Laplacian in a miniature cable, a medium-voltage cable or a full-size cable is a coarse approximation even for reversely calculating conductivity values from leakage current measurements. Using such assumption leads to a wrong understanding of the electric field dependency of the conductivity, and to a wrong estimation of the local current density in the insulation, which are both required for the calculation of the electrical conductivity.

In order to avoid making such approximation, another approach is proposed thereafter to evaluate the material's electrical conductivity: rather than starting by assuming an electric field distribution and then reversely identify the material constants, we propose to calculate the electric field distribution and do the fitting in a common iterative process using both the LMA and the finite element model. This approach will be called LMA-FEM approach.

LMA-FEM approach

In this approach the Levenberg-Marquardt algorithm and the finite-element model are coupled together. This allows taking into account the bidirectional coupling between the conductivity and the electric field: the electric field depends on the conductivity and the conductivity depends on the electric field.

Comsol finite-element calculations are then included directly in the LMA. This results in the block diagram of the Fig. 11, in which the white cases correspond to the LMA and the grey cases are the finite-elements calculations.

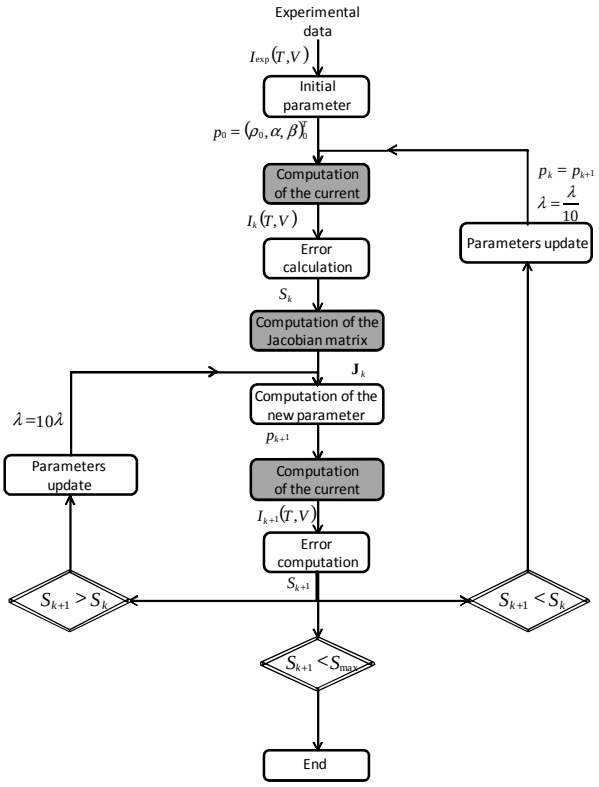

Fig. 11: Block diagram of the LMA-FEM approach

The I(V) curves obtained with this approach are shown on the FIGURE. Even if the values at low electric field still show a poor match with experimental data, the current values obtained for high electric fields now match well.

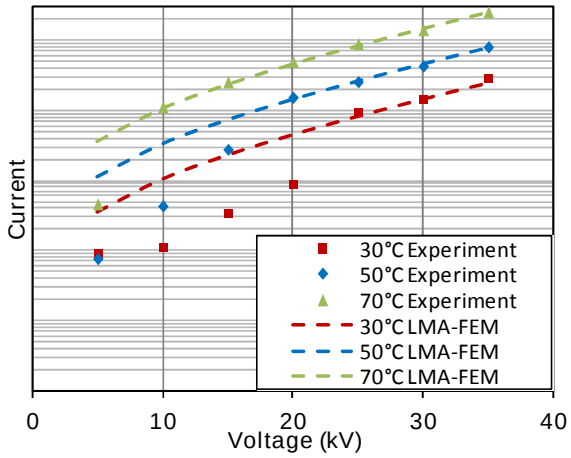

Fig. 12: I(V) curves obtained with the results of the LMA-FEM identification method

The Fig. 13 shows the comparison of the fits obtained with both the usual method and the LMA-FEM method: the LMA-FEM approach results in higher conductivity values, especially for high electric field. Quantitatively speaking, the following differences have been found between the parameters obtained using the standard and the LMA-FEM identification procedures:

$$\Delta\vec{p}_{(LMA-FEM\ /\text{standard})} = \begin{pmatrix} \Delta\sigma_0 \\ \Delta\alpha \\ \Delta\beta \end{pmatrix} = \begin{pmatrix} +22\% \\ -3.4\% \\ +37.5\% \end{pmatrix} \quad [10]$$

Because the temperature was considered homogeneous in the cable, the α temperature coefficient is almost the same. This is an indicator of the stability of the identification algorithm.

On the other hand, significant differences are obtained for the σ_0 and the β parameters. This comes from the fact that the electric field is overestimated in the standard approach, because:

- the maximum "Laplacian" electric field is considered while only a few volume of material close to the conductor is submitted to this field
- the electric field dependency of the electrical conductivity smoothens the electric field, making it more homogeneous and lowering its maximum value

It has been shown that using the average value of the Laplacian electric field across the insulation instead of the maximum value results in conductivity much closer to those obtained by the LMA-FEM approach.

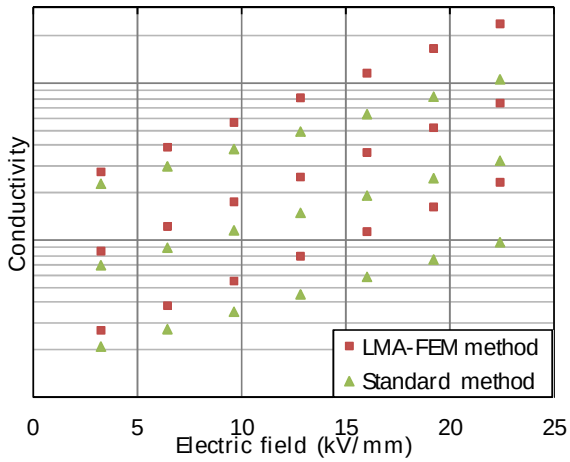

Fig. 13: Comparison of electrical conductivity values obtained by the standard method and by the LMA-FEM approach

This shows the sensitivity of the identification to the way the electric field in the insulation is estimated, and reinforces the need for an algorithm like the LMA-FEM which directly embeds finite-element calculations in the identification procedure.

The problem of the smaller weight of the current values at low electric field in the error function can be overcome by normalizing the errors obtained for each experimental point. It can be showed that this normalization is equivalent to introducing a weight matrix $\mathbf{W}$ in the LMA algorithm, by replacing the equation 9 by the following equation:

$$\vec{p}_{i+1} = \vec{p}_i + \left(\mathbf{J}^T\mathbf{W}\mathbf{J} + \lambda\mathbf{I}\right)^{-1}\mathbf{J}^T\mathbf{W}\left(\vec{I}_{\exp} - \vec{I}_{simul}(\vec{p}_i)\right) \quad [11]$$

Using this weighting method allows obtaining the I(V) curves of the Fig. 14.

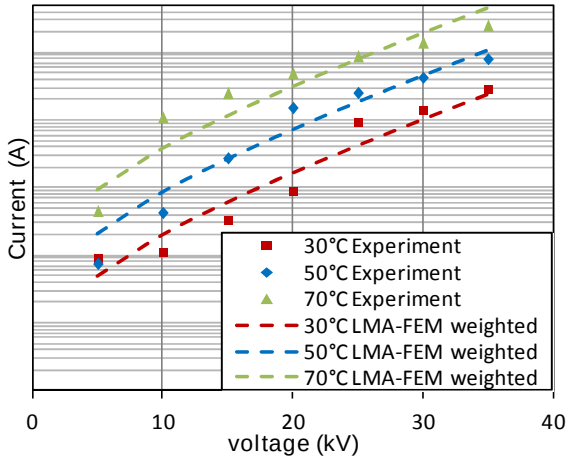

Fig. 14: I(V) curves obtained with the results of the weighted LMA-FEM identification method

It is clear that with this normalization method the low electric field values weight more in the error function. But this is at the cost of a less good fit of the high values. Not being able to obtain a good match for all the experimental data at the same time can have several explanations:

- The experimental data can be wrong for part of the experimental data set: on the Fig. 4, the currents obtained for low electric field values show a lot of noise which significantly reduces the reliability of the obtained data
- The conductivity law does not reflect the actual behaviour of the material. The versatility of this LMA-FEM approach allows easily changing the formulation used for the conductivity. The experimental data set will be confronted to other conductivity formulations in further works, including for instance a contribution of the by-products distribution.

CONCLUSION

A test bench for measuring leakage current on miniature cables has been presented. This test bench allows obtaining leakage currents versus time for different cable temperatures and different voltages with limited bias due to the HV terminations.

It has been shown that, from this experimental data, conductivity values can be obtained using a reverse approach coupling a finite-elements model to the Levenberg-Marquardt optimization algorithm. This approach is very versatile: it allows identifying material constants from any kind of test object, as soon as experimental conditions are known and available. For instance, the finite element model can be enriched with a model of the effect of by-products on the insulation's electrical conductivity.

From the comparison of the results of this LMA-FEM approach with a more standard approach, it is clear that the way the experimental data is used to estimate the electrical conductivity of the material has a huge influence on the final results. Using the LMA-FEM approach is a first step toward more reliable electrical conductivity values. It should be noted that the electrical conductivity values obtained using the standard method are underestimated. Using such values for the design of an HVDC system would result in an overestimation of the system's stability regarding thermal runaway and to a hazardous behavior of the designed system.

The next steps of this work are to experimentally obtain leakage currents from test objects with controlled content of crosslinking by-products: either plates or cable prototypes protected from by-product release to ambient medium could be used. Also, leakage current measurements should be performed at higher voltages to cover the higher electrical field achieved in HVDC cables type-testing.

REFERENCES

[1] Y. Shen, "DC cable systems with extruded dielectrics," *Report*, 2004.

[2] L. Kebbabi, A. Allais, J. Doumbe, and C. Frohne, "Influence of cross-linking by-products on electrical properties of HVDC insulating materials (Relationship between by-products , conductivity and cable dielectric breakdown)," in *JiCable `13*, 2013.

[3] S. a. Boggs, "Semi-empirical high-field conduction model for polyethylene and implications thereof," *IEEE Trans. Dielectr. Electr. Insul.*, vol. 2, no. 1, pp. 97–106, 1995.

[4] D. Fabiani, G.-C. Montanari, L.-A. Dissado, C. Laurent, and G. Teyssedre, "Fast and slow charge packets in polymeric materials under DC stress," in *IEEE Transactions on Dielectrics and Electrical Insulation*, 2009, vol. 16, no. 1, pp. 241–250.

[5] U. Riechert, R. Vogelsang, and J. Kindersberger, "Temperature effect on DC breakdown of polyethylene cables," in *12th International Symposium on High Voltage Engineering*, 2001, pp. 537–540.

[6] M. Fu, L. A. Dissado, G. Chen, and J. C. Fothergill, "Space Charge Formation and its Modified Electric Field under Applied Voltage Reversal and Temperature Gradient in XLPE Cable," *IEEE Trans. Dielectr. Electr. Insul.*, vol. 15, no. 3, 2008.

[7] J. A. Diego, J. Belana, J. Orrit, J. C. Cañadas, M. Mudarra, F. Frutos, and M. Acedo, "Annealing Effect on the Conductivity of XLPE Insulation in Power Cable," *IEEE Trans. Dielectr. Electr. Insul.*, pp. 1554–1561, 2011.

[8] J. C. Fothergill, S. C. Dodd, L. A. Dissado, T. Liu, and U. H. Nilsson, "The Measurement of Very Low Conductivity and Dielectric Loss in XLPE Cables : A Possible Method to Detect Degradation Due to Thermal Aging," *IEEE Trans. Dielectr. Electr. Insul.*, pp. 1544–1553, 2011.

[9] S. Chniba, “Etude des mécanismes de claquage de films de polypropylene dans différents milieux ambiants,” 1984.

[10] C. C. Reddy and T. S. Ramu, “On the Intrinsic Thermal Stability in HVDC Cables,” *IEEE Trans. Dielectr. Electr. Insul.*, vol. 14, no. 6, pp. 1509–1515, 2007.

[11] D. Fabiani, G. C. Montanari, L. A. Dissado, C. Laurent, G. Teyssedre, P. H. F. Morshuis, R. Bodega, A. Campus, and U. H. Nilsson, “Effect of semicon-insulation interface on space charge formation in hvdc polymeric cables,” in *JiCable `07*, 2007.

[12] D. Van Der Born, I. A. Tsekmes, T. J. Person, S. J. Sutton, P. H. F. Morshuis, and J. J. Smit, “Evaluation of space charge accumulation processes in small size polymeric cable models,” *IEEE*, pp. 669–672, 2012.

[13] M. Fu, G. Chen, and J. C. Fothergill, “The Influence of Residue on Space Charge Accumulation in Purposely Modified Thick Plaque XLPE Sample for DC Application H-25,” *Symp. A Q. J. Mod. Foreign Lit.*, pp. 1–6, 2005.

[14] R. Bodega, “Space Charge Accumulation in Polymeric High Voltage DC Cable Systems,” 2006.